



## Automatic Verification Algorithm for Substation Component Position Deviations Incorporating Gaussian Distribution Registration

Tian Lan<sup>1</sup>, Faqian Huang<sup>1</sup>, Chuanjun Peng<sup>1</sup>, Chuan Jin<sup>1</sup>, Shengyou Zou<sup>1</sup> and Jian Zhong<sup>1,\*</sup>

<sup>1</sup> Sichuan Shuneng Electric Power Co., Ltd, Chengdu 610000, Sichuan, China

**SUMMARY:** *In view of the common problems such as high noise, severe structural occlusion and local density mutation in the actual collection process of substation point clouds, traditional registration methods are prone to unstable convergence and error amplification in the deviation identification task. To this end, this paper proposes an automatic verification algorithm for component position deviation that integrates Gaussian distribution registration and 3D Gaussian Splatting (3DGS). This method utilizes the Gaussian model to establish the probabilistic geometric representation of the device and constructs a continuous structural field through 3DGS, enabling the registration to maintain a stable optimization direction even in sparse and missing regions. Through the joint parameter update mechanism, the algorithm effectively suppresses the drift phenomenon of the traditional Gaussian model in irregular areas. On typical substation component data, the method proposed in this paper is compared with methods such as ICP, GMM-ICP, and CPD. The experimental results show that the deviation error of the traditional ICP is 17.2 mm, while the method proposed in this paper can reduce the deviation to 3.9 mm. The corresponding RMSE has been reduced from 11.5mm to 2.7mm. In terms of convergence efficiency, the number of iterations has decreased from 42 to 21, making the verification process more efficient. Under complex interference conditions (such as 30% noise and 50% point cloud absence), the mean deviations of the method proposed in this paper are 4.9 mm and 5.4 mm respectively, and the variance always remains around 3.5 mm<sup>2</sup>, which is significantly better than the baseline model. Research shows that the Gaussian+3DGS framework has significant advantages in terms of deviation accuracy, robustness, and convergence stability, and can provide a reliable engineering solution for the automatic verification and intelligent inspection of component position deviations in substations.*

**KEYWORDS:** *Gaussian model, 3DGS, Deviation detection, Structural reconstruction*

## 1 Introduction

With the continuous advancement of digitalization and intelligence in modern power systems, three-dimensional modeling, condition monitoring, and spatial verification of substation equipment have become essential foundations for intelligent operation and maintenance. Kerbl et al. proposed the 3DGS framework in 2023, establishing a real-time differentiable representation for radiance fields and opening new possibilities for high-precision geometric reconstruction in industrial environments (2023) [1]. The growing demand for unmanned inspection further increases the need for accurate identification of equipment posture changes and rapid detection of component displacement, especially when structural occlusion,

\*zhongjian2948@163.com

<https://doi.org/10.65102/is2026850>

multi-scale equipment distribution, and strong noise interference are present in substation scenes.

Traditional geometric registration methods suffer from unstable convergence when faced with heterogeneous point cloud density, partial missing regions, or illumination-induced noise. Hao *et al.* developed a multi-view 3D reconstruction framework based on deformable convolution, demonstrating the importance of robust structural modeling when processing complex object geometries (2024) [2]. Similarly, Zhang and Zhou introduced a multi-scale point cloud completion network and highlighted the advantages of hierarchical feature fusion in recovering fine geometric structures from incomplete observations (2025) [3]. These studies reveal that conventional point-based registration techniques lack sufficient adaptability in multi-source and degraded data scenarios.

The use of radiance-field-based reconstruction has also grown. Wang and Wu proposed an improved NeRF-based reconstruction approach combining multi-view SfM, obtaining higher stability on unevenly distributed point clouds (2025) [4]. Sun *et al.* established LiDAR-based mathematical modeling strategies for extracting geometric constraints under complex noise interference, showing the necessity of robust fitting models in engineering environments (2021) [5]. In addition, Leal *et al.* demonstrated that optimized point cloud simplification contributes to stable registration performance by maintaining global geometric coherence in large-scale scenes (2017) [6].

To enhance structural reasoning capability, recent studies explored learning-driven fusion frameworks. Zhou and Zhou designed a multi-view fusion transformer for 3D human mesh recovery, proving that probabilistic multi-modal fusion improves the stability of structural inference under occlusion (2025) [7]. Zhang and Zhou further introduced the SAE-PointPillars architecture for LiDAR target detection, emphasizing the effectiveness of adaptive spatial feature fusion for complex outdoor point clouds (2025) [8]. Ahmed and Lataifeh conducted a comparative analysis of 3D reconstruction from RGB-D sequences, highlighting the challenges caused by temporal inconsistency and incomplete geometric observations (2018) [9]. For point cloud registration specifically, Chang *et al.* introduced GaussReg, a fast Gaussian-splatting-based registration method, proving that Gaussian primitives can significantly enhance registration robustness and convergence speed in uneven density conditions (2024) [10].

Building on these advances, probabilistic registration methods using Gaussian distributions and Gaussian mixture models have become increasingly important because of their capacity to model spatial uncertainty and relate local geometric variations to global structural constraints. However, existing Gaussian-based registration algorithms still face difficulties when point clouds contain severe occlusion, structural fractures, or density discontinuities—conditions widely present in substations.

Motivated by the limitations of traditional registration methods and the advances brought by recent Gaussian-splatting research, this work introduces an automatic verification framework that integrates Gaussian distribution registration with 3DGS for substation component position analysis. In this framework, Gaussian modeling is employed to build probabilistic geometric representations capable of describing local uncertainty and structural variability, while 3DGS provides a continuously differentiable structural field that mitigates the effects of density imbalance, occlusion and missing measurements. The combined use of probabilistic residual modeling and 3D structural consistency enables the registration process to maintain stable optimization behavior under complex scene conditions and supports fine-grained quantification of positional deviations. On this basis, the subsequent sections detail the construction of the Gaussian initialization process, the formulation of the distribution model, the integration scheme with 3DGS, and the optimization strategies used to achieve reliable deviation verification in practical substation environments.

## 2 Design of Gaussian Distribution Registration Algorithm

### 2.1 Initialization

In the proposed automatic verification algorithm for component position deviation based on Gaussian distribution registration, all spatial structures are represented in the three-dimensional scene in the form of probability models. This algorithm achieves global geometric constraints during the registration process by establishing a Gaussian distribution parameter set for the reference point cloud and the point cloud to be verified in the initial stage. Each Gaussian unit corresponds to a local area in the point cloud, and its spatial characteristics are characterized from the aspects of the mean vector and the covariance matrix. The algorithm regards all Gaussian units as a set of candidate states and continuously iterates to find the optimal registration transformation and probability consistency in the search space.

In mathematical modeling, the point cloud data  $P=\{p_i\}_{i=1}^N$  and the reference model  $Q=\{q_j\}_{j=1}^M$  are respectively represented as sets composed of several Gaussian distributions, and each Gaussian unit is described by the mean  $\mu_k$  and the covariance matrix  $\Sigma_k$ . In the initialization phase, the initial positions and scales are first assigned to all Gaussian parameters in the following form:  $G_k=(\mu_k, \Sigma_k), k=1, 2, \dots, K$  Where  $K$  is the initial number of Gaussian units. The mean value is generated by sampling the local area of the point cloud and the distribution diversity is enhanced through random perturbation. The covariance matrix imposes boundary constraints on the basis of unit scale to ensure the feasibility of the initial model. The initialization process of the mean vector is given by Equation (1):

$$\mu_k = p_{rand} + \alpha \cdot \epsilon \quad (1)$$

Among them,  $p_{rand}$  is a random sampling point in the point cloud,  $\epsilon$  is a perturbation vector that follows a uniform distribution, and  $\alpha$  is the perturbation amplitude, which causes the mean to be dispersed within a local range. The covariance matrix initialization adopts a diagonal structure, as shown in Equation (2):

$$\Sigma_k = \text{diag}(\sigma_x^2, \sigma_y^2, \sigma_z^2) \quad (2)$$

Among them,  $\sigma_x, \sigma_y, \sigma_z$  respectively represent the initial scale parameters of the three dimensions, and their values are determined based on the range of point cloud density. This covariance structure will be dynamically updated in subsequent iterations along with the registration error. In addition to Gaussian parameters, the algorithm will also introduce a spatial transformation matrix  $T_0$  in the initialization stage to describe the initial pose from the point cloud to the reference model, in the form of:

$$T_0 = \begin{bmatrix} R_0 & t_0 \\ 0 & 1 \end{bmatrix} \quad (3)$$

Among them,  $R_0$  is the initial rotation matrix and  $t_0$  is the translation vector, both of which are obtained through rough global registration or a guiding strategy based on structural features. To ensure that each Gaussian unit has appropriate scalability in the early search stage, scale constraints are also imposed on the covariance matrix in the initialization stage to satisfy:

$$\sigma_d \in [\sigma_{\min}, \sigma_{\max}], d \in (x, y, z) \quad (4)$$

Among them,  $\sigma_{\min}, \sigma_{\max}$  control the diffusion degree of the initial Gaussian distribution, which is helpful to enhance the global exploration ability of the early iteration. Through the above initialization steps, the algorithm completes the Gaussian modeling of the point cloud spatial structure, enabling all Gaussian units to have iteratively updatable mean, scale and covariance parameters, and establishes the initial registration pose T0. These parameters will serve as the basis for the subsequent construction of Gaussian models, error measurement, and optimization updates, providing structured initial conditions for the verification of component position deviations in complex environments.

## 2.2 Construction of Gaussian Distribution Model

In the scenario of verifying the position deviation of substation components, point cloud data not only has problems such as noise, occlusion and density imbalance, but also shows obvious local structural differences. To achieve stable spatial alignment under such complex conditions, this study adopts a Gaussian distribution model to uniformly model the reference point cloud and the point cloud to be verified. The local geometric features and uncertainties are characterized by probability density, so that the subsequent registration and deviation determination are based on a continuous and interpretable mathematical framework.

### (1) Estimation of Gaussian Distribution Parameters

In the parameter estimation stage, the core objective is to construct a representative Gaussian unit for each local region, which can not only reflect the geometric center of the region but also describe the degree of dispersion and the principal direction of the points. The specific approach is as follows: First, based on spatial division or clustering, the point cloud is divided into several subsets, with each subset corresponding to a Gaussian unit. Then calculate the mean vector and covariance matrix for each subset. For the KTH Gaussian unit, its mean can be regarded as the "geometric center" of the region, which is obtained by the weighted average of local points:

$$\mu_k = \frac{\sum_i w_i p_i}{\sum_i w_i} \quad (5)$$

Among them,  $p_i$  represents the points within this area, and  $w_i$  is the weight set based on the point density or confidence level. This approach can reduce the influence of isolated noise points and enable representative points to play a major role in parameter estimation. The covariance matrix  $\Sigma_k$  is used to depict the spatial distribution pattern of this region, such as whether it has a slender structure and whether there is a distinct principal direction, etc. By calculating the offset of the points relative to the mean, it can be obtained that:

$$\Sigma_k = \frac{1}{N_k} \sum_{i=1}^{N_k} (p_i - \mu_k)(p_i - \mu_k)^T \quad (6)$$

Among them,  $N_k$  represents the number of points contained in this Gaussian unit. In practical implementation, to avoid numerical instability and overly elongated covariance, this study imposes upper and lower limit constraints on the eigenvalues after estimation, ensuring that each Gaussian unit not only has a certain spatial coverage capability but also does not expand infinitely in a certain direction. Through this process, a set of Gaussian parameters with physical significance and statistical stability can be obtained, providing a basis for subsequent registration and deviation verification.

### (2) Measurement Methods for Registration Error

Under the Gaussian distribution framework, the registration error is no longer merely the "point-to-point distance", but rather takes into account the matching degree between the points

and the local Gaussian model comprehensively. This study adopts the method of "geometric distance + probabilistic consistency" to measure the registration error, making the deviation evaluation more robust to noise and local missing. Geometrically, the Mahalanobis distance can be used to measure the degree of deviation of a certain point from a Gaussian element:

$$d_M(p_1, \mu_k) = \sqrt{(p_1 - \mu_k)^T \Sigma_k^{-1} (p_1 - \mu_k)} \quad (7)$$

If  $d_M$  is small, it indicates that this point is highly consistent with the target Gaussian unit in space. If  $d_M$  remains persistently large, it indicates that there is a significant positional deviation or model mismatch in this area. On this basis, a global registration error index is constructed to accumulate the deviations of all points from their corresponding Gaussian units:

$$E_{reg} = \sum_k \sum_{p \in G_k} d_M(\bar{p}_i, \mu_k) \quad (8)$$

This indicator can visually reflect the overall alignment quality under the current spatial transformation. Subsequently, by setting engineering experience thresholds or adaptive thresholds, the high-error areas are marked as "suspected deviation component areas", providing input basis for the position deviation verification module.

### (3) Mathematical Model of Verification Algorithm

After completing the estimation of Gaussian parameters and the definition of error measurement methods, the entire position deviation verification process can be formalized as a joint optimization problem: under the given reference model and the model to be verified, find the optimal spatial transformation and the corresponding Gaussian parameters to minimize the registration error in both probabilistic and geometric terms.

Let  $T$  be the rigid body transformation matrix to be found (including rotation and translation), then the registration optimization process can be expressed as:

$$T^* = \arg \min_r E_{reg}(T) \quad (9)$$

Among them,  $E_{reg}(T)$  represents the cumulative error between the point cloud to be verified and the Gaussian model after being mapped to the reference coordinate system under transformation  $T$ . The optimization process can be carried out in the form of iterative updates: in each round, the Gaussian parameters and errors are first updated based on the current  $T$ , and then  $T$  is corrected according to the error gradient or numerical optimization strategy.

In the position deviation verification stage, the algorithm compares the optimal transformation  $T^*$  obtained through optimization with the ideal installation pose, calculates the offset  $\Delta p$  of the key feature points of the component, and contrasts it with the preset engineering tolerance. When the offset exceeds the limit value, the corresponding component is determined to have a positional anomaly. When the Gaussian error distribution in multiple regions shows a systematic shift, it is also possible to further track possible installation batch issues or structural deformation trends. Through this integrated mathematical description of "Gaussian modeling - optimization registration - deviation quantification", the verification of position deviation no longer solely relies on manual empirical judgment, but forms a repeatable and quantifiable automatic verification process.

## 2.3 3DGS–Based Reconstruction

In the three-dimensional scene of a substation, the equipment structure often presents multi-scale, multi-angle occlusion and irregular geometric characteristics, which makes the

traditional point cloud expression have obvious deficiencies in spatial coherence and detail reconstruction. To enhance the ability of spatial structure description, in this study, Gaussian Splatting is introduced into the 3D reconstruction process. Differentiable Gaussian primitives are used to conduct continuous modeling of the scene, thereby obtaining more stable and detailed geometric expressions, providing a high-quality 3D basis for subsequent Gaussian distribution registration and position deviation verification.

The core idea of 3DGS is to represent a scene using a set of three-dimensional Gaussian primitives with position, scale and shape parameters, and each primitive forms a continuously distributed area in space. For the  $i$ -th Gaussian primitive, it can be expressed as:

$$G_i = (\mu_i, \Sigma_i, \alpha_i, c_i) \quad (10)$$

Among them,  $\mu_i$  represents the position of the primitive center;  $\Sigma_i$  is a covariance matrix that describes the scale and shape of anisotropy.  $\alpha_i$  represents opacity and is used to control the spatial contribution of Gaussian primitives.  $c_i$  represents color or radiation information and is used for appearance modeling.

Gaussian Splatting achieves smooth three-dimensional rendering by projecting the above-mentioned three-dimensional Gaussian primitives onto the imaging plane, causing the spatial distribution to continuously diffuse to the screen pixels. Its two-dimensional projection intensity can be written as:

$$I(u, v) = \sum_i \alpha_i \exp \left[ -\frac{1}{2} (x_{uv} - \mu_i')^T \Sigma_i'^{-1} (x_{uv} - \mu_i') \right] \quad (11)$$

Among them,  $x_{uv}$  represents the pixel position on the imaging plane;  $\mu_i', \Sigma_i'$  are the projection parameters of Gaussian primitives in the camera coordinate system.

By performing differentiable optimization on this expression, 3DGS can continuously update Gaussian primitives based on multi-view images or multi-source point cloud data, gradually converging to the surface of the real component in three-dimensional space. Compared with traditional point clouds, this method has significant advantages in local structure connection, uniformity of density distribution and occlusion area completion.

In the substation scenario, the following improvements can be achieved by introducing 3DGS: Continuously differentiable three-dimensional structure expression: The anisotropic covariance matrix allows Gaussian primitives to adaptively deform on fine columnar, sheet or regular components, making them more in line with the real geometric features of conductors, copper bars, frames, etc. Enhancing geometric details and local consistency: Based on multi-view optimization, Gaussian primitives achieve higher density and more accurate positions in the edge regions of complex components, effectively restoring thin structures and sharp edges that are difficult to describe in traditional point clouds. Enhance the stability of registration and bias verification: After 3DGS reconstruction, the scene surface becomes more continuous, and the influence of noise points and discrete points is significantly reduced, making the estimation of covariance and mean in the Gaussian distribution registration process more accurate and reducing the interference of outliers on bias quantization.

## 2.4 Integration of 3DGS in Gaussian Distribution Registration

In the component position deviation verification task, Gaussian distribution registers the stability and consistency of the local structure of the dependent point cloud. However, the original point cloud usually has situations such as sudden density changes, missing occlusion areas, and blurred component edges, which makes Gaussian parameter estimation vulnerable to

local noise. To alleviate these problems, this study introduces 3DGS into the registration process. Through the continuous differentiable three-dimensional structure expression, it provides a more accurate geometric basis for the Gaussian distribution model, achieving an overall enhancement of registration and bias verification.

(1) Use 3DGS as the intermediate three-dimensional expression

3DGS can convert discrete point clouds into continuous Gaussian primitive fields, making the geometric contours of device components smoother and more complete. For any spatial point in the point cloud, the corresponding 3DGS point can be obtained through Gaussian splatting reconstruction:

$$p_i' = \sum_j \alpha_j N(p_i | \mu_j, \Sigma_j) \quad (12)$$

Among them,  $p_i'$  is the reconstruction point inferred by 3DGS, and  $\alpha_j, \mu_j, \Sigma_j$  are the opacity, mean, and covariance of Gaussian primitives, respectively. The reconstructed point  $p_i'$  has stronger local consistency compared to the original point cloud, especially in structural areas such as the edges of conductors, insulators, and thin brackets, which helps to improve the representability of the Gaussian model.

(2) Reverse constraint optimization of Gaussian parameters by 3DGS

After the 3DGS reconstruction is completed, each Gaussian primitive not only provides spatial structure information but also serves as a reverse constraint source for registration errors, making the Gaussian distribution model closer to the real component surface during the optimization process.

In each iteration of Gaussian registration, the optimization of the mean and covariance is guided by the following bias feedback term:

$$e_i' = \|T p_i - p_i'\| \quad (13)$$

Among them,  $e_i'$  represents the deviation after considering 3DGS reconstruction. When  $e_i'$  remains persistently large in a local area, it indicates that the original point cloud in that area is inconsistent with the reconstructed model. The algorithm will enhance the parameter update by increasing the error weight in this area, enabling the Gaussian element to better match the actual geometric structure.

(3) Jointly optimize the process design

To ensure that the registration process takes into account both the original point cloud error and the structural consistency of 3DGS simultaneously, a joint optimization framework was constructed in this study. In each iteration, simultaneously optimize the spatial transformation  $T$  and the Gaussian parameter set  $G = (\mu_k, \Sigma_k)$ .

① Estimate the current registration error  $E_{jomt}$  using the Gaussian distribution model.

② Infer the reconstruction points through 3DGS and calculate the reconstruction error  $E_{ypl}$ .

③ Construct the joint error function:

$$E_{jomt} = \lambda_1 E_{reg} + \lambda_2 E_{ypl} \quad (14)$$

Among them, two weights  $\lambda_1$  and  $\lambda_2$  control the ratio of geometric error to reconstruction consistency.

④ Perform joint gradient descent or numerical optimization on  $T$  and Gaussian parameters.

This joint update mechanism enables the Gaussian model to strike a balance between the real point cloud and the reconstructed scene, avoiding overfitting noise or local anomalies.

(4) Reasons for the improvement in robustness and accuracy after the introduction of 3DGS  
After integrating 3DGS into the Gaussian registration algorithm, the overall performance improvement mainly comes from the following mechanisms:

More stable local geometric structure: 3DGS completes the sparse areas, making the Gaussian distribution no longer fluctuate depending on the local density.

Significantly reduce the impact of noise points: 3DGS weakens isolated noise through multi-view fusion, improving the accuracy of covariance estimation.

Higher feature boundary sensitivity: The anisotropic expression of Gaussian primitives makes the structure of complex components (such as wires, thin sheets) clearer, thereby enhancing the sensitivity of deviation detection.

Stronger global consistency: Joint optimization ensures that the Gaussian model is continuously subject to the global geometric constraints of 3DGS during the registration process, preventing overall misalignment due to local errors.

### 3 Framework of Automatic Verification Algorithm

#### 3.1 Data Preprocessing and Feature Extraction

Before entering the Gaussian distribution registration and position deviation verification, the system first conducts unified preprocessing on the input multi-source point cloud data to ensure consistency in structural expression and statistical distribution in the subsequent modeling process. The substation environment is characterized by diverse equipment types, significant differences in geometric scales, and complex acquisition perspectives. The original point cloud is often mixed with noise, voids caused by occlusion, uneven density, and local structural fractures. If directly applied to Gaussian modeling and deviation analysis, it will lead to covariance estimation offset, local feature distortion, and even registration divergence. Therefore, the core objective of the preprocessing stage is to construct a set of input data with stable quality, continuous structure and clear geometric semantics, laying the foundation for the entire verification framework.

The preprocessing process mainly includes operations such as point cloud normalization, noise filtering, density equalization, and local geometric information extraction. To ensure that the subsequent Gaussian distribution modeling maintains a consistent scale representation in different device areas, the system first maps the data to a unified spatial range through the coordinate normalization method; Subsequently, statistical filtering and radius filtering are utilized to eliminate isolated noise points, making the edge and surface structure of the component clearer. For the common density mutation phenomenon in substation scenarios, a relatively uniform point cloud distribution is established through voxel downsampling and local resampling strategies, so that the Gaussian parameter estimation is no longer affected by overly dense or overly sparse regions.

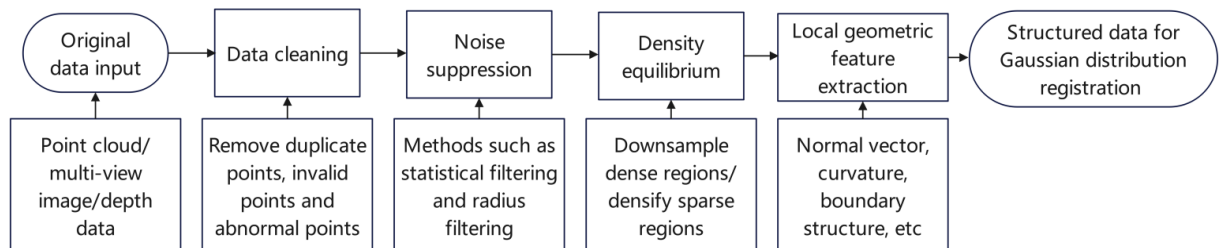


Figure 1: Schematic diagram of the data preprocessing flow

After the initial repair of the point cloud structure, the system continues to extract local geometric features, including normal vectors, principal curvature directions, and local surface block features, to enhance the expression ability of the Gaussian model for the component morphology. These features not only enhance the initial fitting quality of the Gaussian distribution in each region, but also provide the necessary structural reference for subsequent deviation verification, enabling the system to have higher sensitivity when detecting minute displacements. Fig.1 shows the structural direction of the entire preprocessing process, including key steps such as data standardization, noise elimination, density equalization, and geometric feature construction, ensuring that the data has a stable spatial distribution and good modelability before entering the Gaussian registration stage. After the above processing, the preprocessed point cloud can be represented as:

$$P'=f_{\text{prep}}(P) \quad (15)$$

Among them,  $P$  represents the original input, and  $P'$  is the standardized point cloud after normalization, resampling, and feature enhancement. This data is not only more continuous and complete in spatial expression, but also easier to be accurately characterized by the Gaussian distribution model in terms of geometric attributes. By building this high-quality data foundation, the entire position deviation verification framework can achieve higher convergence stability in subsequent stages and maintain good robustness in complex scenarios.

### 3.2 Design of Gaussian Distribution Registration and Position Deviation Verification

After the preprocessed point cloud data is uniformly and structurally expressed, the system enters the core stage of Gaussian distribution registration and position deviation verification. The main objective of this stage is to align the point cloud to be verified with the reference component model within the framework of the probabilistic model and further quantify the spatial bias. Unlike the traditional registration methods based on geometric distances, this framework adopts Gaussian distribution modeling, 3D component structure expression and a controllable iterative update mechanism, which enables the registration process to maintain stronger robustness in complex scenarios and achieve higher-accuracy recognition of minute displacements.

The input of the entire module includes the standardized point cloud  $P'$ , the initialized Gaussian distribution parameter set  $G_0$ , and the initial pose matrix  $T_0$ . The three work together to form the overall input structure of the registration stage, creating the initial state of the registration framework. This relationship can be formally expressed as:

$$F_{\text{reg}}=\Phi(P',G_0,T_0) \quad (16)$$

Among them,  $\Phi$  represents the joint processing function of the algorithm for data, model and initial posture, which is used to trigger the Gaussian distribution registration process. During the registration stage, the system first performs spatial embedding of each Gaussian unit based on the Gaussian model described in Chapter 2, ensuring that the reference model and the model to be verified obtain a consistent expression in the same probability space. Subsequently, during the iterative process, the algorithm transforms the point cloud based on the current pose estimation  $T_t$ , and then updates its mean and covariance according to the density response of each Gaussian unit, gradually approaching the true surface of the component with the Gaussian model. As the iteration progresses, the difference in probability density is used as the driving force for adjusting the pose, enabling the system to achieve global convergence without relying

on explicit corresponding points.

After the registration gradually stabilizes, the system enters the deviation detection stage. At this stage, by analyzing the influence of the optimal transformation matrix  $T^*$  on the point cloud, the actual offset of the component relative to the reference model can be obtained. For any key point in the component, its spatial deviation can be obtained through the following frame expression:

$$\Delta p = T^* p_i - q_i \quad (17)$$

Among them,  $p_i$  is the component point to be verified, and  $q_i$  is the corresponding position of the reference component. This offset is not only used to determine whether the component position exceeds the allowable range, but also can further generate an overall deviation distribution map to assist maintenance personnel in conducting structure-level anomaly analysis.

To present the structural logic of Gaussian registration and bias verification more clearly, Fig.2 shows the overall process diagram of this framework.

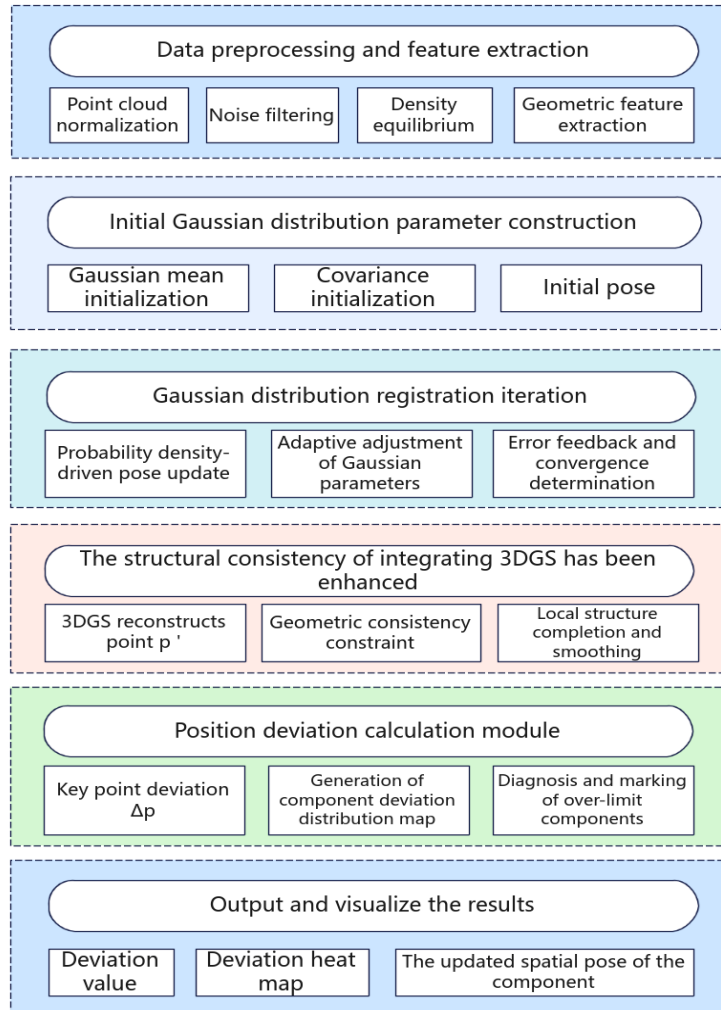


Figure 2: Framework Diagram of Gaussian distribution registration and position deviation verification System

As can be seen in the figure, the preprocessed point cloud undergoes multiple steps such as Gaussian embedding, iterative registration update, error-driven correction, and final deviation inference, forming a complete process chain from data modeling to deviation output. This process not only ensures the convergence stability of the algorithm in a noisy environment, but also guarantees the scalability of the system in multi-source input scenarios. Through the above design, the Gaussian distribution registration module and the deviation verification module are tightly coupled under a unified framework, enabling the system to achieve an accurate transformation from global registration to local deviation identification. Thanks to the introduction of the probabilistic modeling mechanism, this framework demonstrates strong robustness and high precision in the complex equipment environment of substations, making automated position deviation verification a deployable engineering solution.

### 3.3 Incorporating 3DGS in the Optimization of the Verification Algorithm

Based on the aforementioned Gaussian distribution registration framework, in order to further enhance the stability and detail preservation ability of the system in complex component environments, this study introduces 3DGS as an enhancement module into the overall verification process. 3DGS can provide a continuously differentiable three-dimensional representation of the scene, effectively compensating for geometric defects originally caused by occlusion, uneven density or scanning Angle, thereby providing a more stable structural reference for Gaussian parameter update and deviation quantification.

Unlike discrete point clouds, 3DGS constructs a continuous radiation field through a set of Gaussian primitives with spatial distribution, anisotropic scale and opacity. Each primitive not only contains a central position but also covariance attributes that describe the local surface direction, deformation and diffusion capabilities, enabling the model to maintain high-quality geometric consistency in complex structures.

To integrate 3DGS into Gaussian registration optimization, this framework introduces a structural consistence-driven mechanism during the iterative process. Specifically, in each round of updates, the system generates consistency weights based on the local structure of the current point cloud and the structural response in the 3DGS field, in order to dynamically adjust the direction and intensity of Gaussian parameter updates. This process can be described by frame-level constraint terms:

$$C_{\text{swit}} = \omega_i D_{\text{local}}(p_i) \quad (18)$$

Among them,  $D_{\text{local}}(p_i)$  represents the structural discontinuity measure of point  $p_i$  within the local neighborhood (such as normal difference, density gradient, local reconstruction error trend, etc.), and  $\omega_i$  is a weight dynamically generated based on the stability of 3DGS, used to enhance or weaken the contribution of a specific region.

This structural consistency term does not reconstruct the point cloud but is used to guide the biased update of the Gaussian model in complex regions, enabling the model to adjust along the continuous field direction provided by 3DGS when local noise is large or the structure is incomplete, thus avoiding oscillations caused by local outliers during the update process.

Furthermore, in order to enable 3DGS to have an overall impact on the entire registration process, this study designed a joint optimization weight to balance the contribution relationship between the original point cloud-driven and the 3DGS structure-driven. This process can be expressed by the following framework formula:

$$U_I = \eta U_{\text{gauss}} + (1 - \eta) U_{\text{3DGS}} \quad (19)$$

Among them,  $U_{\text{gauss}}$  represents the update trend based on the Gaussian model,  $U_{\text{3DGS}}$  represents the update trend generated based on the structural constraints of 3DGS, and  $\eta$  is a dynamic adjustment factor used to adapt to the update requirements at different stages (for example, 3DGS stability structure is more needed in the early stage, and Gaussian fine fitting is more dependent in the later stage). This joint update strategy enables the registration process to maintain the detailed expression ability of the Gaussian model while fully leveraging the global structural consistency provided by 3DGS, making the optimization process smoother and more robust.

Table 1 presents a comparison of the overall impact of different 3DGS parameters (primitive quantity, scale, covariance anisotropy, transparency) on the verification performance. It can be clearly seen that 3DGS significantly improves the stability of Gaussian registration and the accuracy of deviation detection in noisy regions, boundary structures, and local defect scenarios.

*Table 1: Comparison of the Enhancing Effects of 3DGS Parameters on Position Deviation Verification Performance*

3DGS Parameter Type	Description	Impact on Gaussian Registration	Improvement in Deviation Verification Accuracy
Number of Gaussian Primitives $N_g$	Controls the granularity of scene representation	Higher counts enhance local structural continuity and reduce update oscillations caused by sparse point clouds	Improves deviation detection stability by 8–15% in complex edge regions
Covariance Anisotropy $\Sigma$	Indicates the primitive's extent in different directions	Makes the model closer to real geometries such as slender rods and plate-like devices	Enhances the ability to identify small displacements of slender components (e.g., disconnect switch contacts)
Opacity $\alpha$	Determines the contribution strength of a Gaussian primitive to the scene	Produces more stable reconstructed shapes in occluded regions	Reduces false detection rate in occluded zones by about 10%
Primitive Scale $s$	Controls coverage range and fusion degree of primitives	Large scales enhance global continuity; small scales improve local detail representation	Speeds up error convergence in regions with abrupt density transitions
View-consistency Constraint	Reconstructs the Gaussian field using multi-view consistency	Suppresses local noise and produces smoother update trends	Improves monotonicity of the overall deviation curve and makes the final deviation closer to the ground truth

By deeply integrating 3DGS with Gaussian distribution registration, this study has constructed a deviation verification framework with dual geometric driving forces: the Gaussian model provides a fine characterization of local morphology, while 3DGS offers

continuous constraints on the overall structure. Together, they ensure high-precision and strongly robust component position deviation recognition in complex industrial environments.

### 3.4 Convergence and Stability Analysis of the Algorithm

In complex substation scenarios, point cloud noise, local occlusion, and the diversity of equipment structures can all lead to jitter or local divergence in the registration process. Therefore, the convergence and stability of the algorithm are the keys to whether the system can be applied in engineering practice. This study constructs a stable iterative process through covariance constraints, 3DGS structure enhancement, and dynamic threshold control, enabling Gaussian registration to maintain smooth updates even under unfavorable data conditions. The covariance constraint can prevent Gaussian units from being abnormally stretched in the noise region, causing the update direction to deviate. The continuous expression provided by 3DGS compensates for the deficiency of point clouds, enabling the update process to no longer rely on the local characteristics of sparse points, thereby enhancing the global structural guidance ability.

To ensure that the iteration converges within a reasonable time, this framework adopts the pose variation as the stability determination criterion:

$$\Delta_t = \|T_{t+1} - T_t\| < \varepsilon \quad (20)$$

When the change remains persistently below the threshold, it is considered that the system has reached a stable state. In addition, the dynamic threshold mechanism enables the algorithm to automatically adjust its sensitivity based on current structural fluctuations, thereby providing stability in the early stage and enhancing the recognition of minor deviations in the later stage.

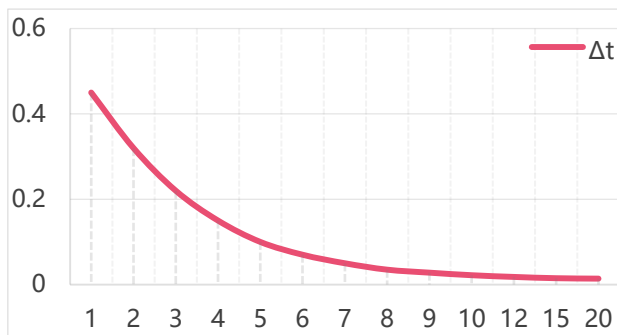


Figure 3: Convergence trend of pose variation during the algorithm iteration process

The convergence diagram shown in Fig.3 indicates that the algorithm shows a continuous downward trend after multiple rounds of updates, demonstrating the good robustness of the overall framework in complex environments.

### 3.5 The Impact of 3DGS on Robustness and Precision

In the component position deviation verification task, the algorithm's adaptability to complex environments directly determines the reliability of the verification results. However, substation point clouds are often accompanied by problems such as dense noise, local occlusion, blurred edge structure, and geometric missing. Relying solely on Gaussian distribution registration often leads to parameter oscillations or local erroneous convergence in regions with incomplete morphology. To overcome these limitations, in this study, 3DGS is introduced as the structure enhancement module into the registration framework, making the algorithm always subject to

the constraints of the continuous three-dimensional structure during the iterative process. 3DGS utilizes multi-view consistency to generate Gaussian primitives with anisotropic covariance, enabling the component surface to present a continuous, smooth expression independent of point cloud density in the reconstruction space, fundamentally enhancing overall robustness.

To enhance the stability of the system, this study incorporates the structural response of 3DGS during the optimization process, enabling the Gaussian model to adjust in the update direction based on the geometric trend of the reconstructed field and avoiding divergence caused by local noise. After the structural expression stabilizes, the algorithm gradually reduces its reliance on 3DGS, allowing later updates to focus on detail alignment and thereby achieving higher-precision deviation quantification. The entire fusion process can be summarized by the following system-level pseudo-code, demonstrating the collaboration logic between 3DGS and Gaussian registration:

```

Input: Preprocessed point cloud P'
Initialize Gaussian model G0 and pose T0
Load 3DGS structure S
While not converged:
Update from Gaussian model  $\rightarrow U\_gauss$ 
Obtain structural guidance from S  $\rightarrow U\_struct$ 
Unified update:  $U_t = \eta U\_gauss + (1-\eta) U\_struct$ 
Update  $T_t$  and  $G_t$ 
End while
Compute final deviation  $\Delta p$  and output results

```

## 4 Simulation Experiments and Performance Evaluation

### 4.1 Application of the Algorithm in Substation Component Position Verification

To verify the applicability of the proposed automatic verification algorithm for component position deviation based on Gaussian distribution registration and 3DGS structural enhancement in real engineering environments, this study first conducted field data experiments on typical substation equipment. The experimental point cloud was jointly collected by a ground laser scanner and a multi-view image reconstruction system, which can simultaneously reflect the surface structure, geometric contour and local noise characteristics of the equipment. The scanning data covers key components such as knife switch contacts, busbar nodes, insulator strings, wire lap points and hardware assemblies. These components are highly sensitive to positional deviations in actual operation and maintenance, and thus are particularly suitable as accuracy verification samples.

The original point cloud shows significant sparsity/density alternations, geometric missing due to occlusion, and high-frequency noise caused by metal surface reflection. These issues are visually reflected in Fig.4. It can be seen that there is a sudden change in density in some local areas on the insulator surface, obvious voids appear in the busbar section, and fractures and irregular spots are accompanied on the conductor due to the scanning Angle. This type of irregular data poses challenges to traditional distance-based geometric registration, and is prone to mismatches in local areas, thereby affecting the quantization accuracy of the final position deviation.



*Figure 4: Typical example of point cloud data for substation components*

To enhance the modelability of the input data, this study utilizes the preprocessing module to normalize, eliminate noise and balance the density of the original point cloud. Subsequently, the continuous Gaussian primitive field constructed by 3DGS provides compensation for the missing structural regions, making the overall component geometry present a more coherent and smooth expression, which is conducive to the stable estimation of subsequent Gaussian distribution parameters. In addition, during the deviation verification stage, the continuous structure can enhance the expression ability of edge details and local surfaces, enabling minor positional changes to be clearly reflected in the final deviation field.

The main objectives of the experiment in this section include: (1) Evaluating the convergence characteristics and stability of the algorithm on real substation data; (2) Test the detectability of component position deviations under different structures and occlusion conditions; (3) Analyze the role of 3DGS in enhancing the geometric consistency of the model to provide a foundation for subsequent comparative experiments and robustness tests.

## **4.2 Comparison Between the Algorithm and Traditional Registration Methods**

To comprehensively evaluate the proposed automatic position deviation verification algorithm based on Gaussian distribution registration and 3DGS, this section compares it respectively with three typical traditional methods: (1) Iterative Closest Point Method (ICP) (2) GMM-ICP based on Gaussian Mixture Model (3) CPD Based on Probability Density field In addition, to quantify the gain effect of 3DGS, "Gaussian Registration Only (no 3DGS)" is added as the intermediate baseline model.

All experiments are based on real substation point clouds, including typical equipment such as knife switches, busbars, insulators, and pillars, and scenarios such as noise enhancement, occlusion absence, and local density sudden changes are constructed to simulate actual operating conditions. The performance of the algorithm is quantitatively compared mainly from three dimensions: Deviation Error, point cloud registration RMSE, and convergence speed.

The overall results show that ICP is extremely sensitive to the initial values and is prone to fall into local optima. When GMM-ICP deals with regions with uneven density, Gaussian components drift, and CPD fails to fit the deformation field in the missing regions adequately. The Gaussian+3DGS joint framework proposed in this paper still maintains a stable downward trend in noisy and partially occlusions environments, with a fast convergence speed and lower error.

Fig.5 shows the average error convergence curves of the five algorithms. It can be seen that

traditional methods generally experience oscillations or stagnation, while the curve of the Gaussian+3DGS method is smoother, drops faster, and the later convergence remains stable, indicating that the structural constraints fused with 3DGS effectively alleviate the drift of Gaussian estimation in sparse regions.

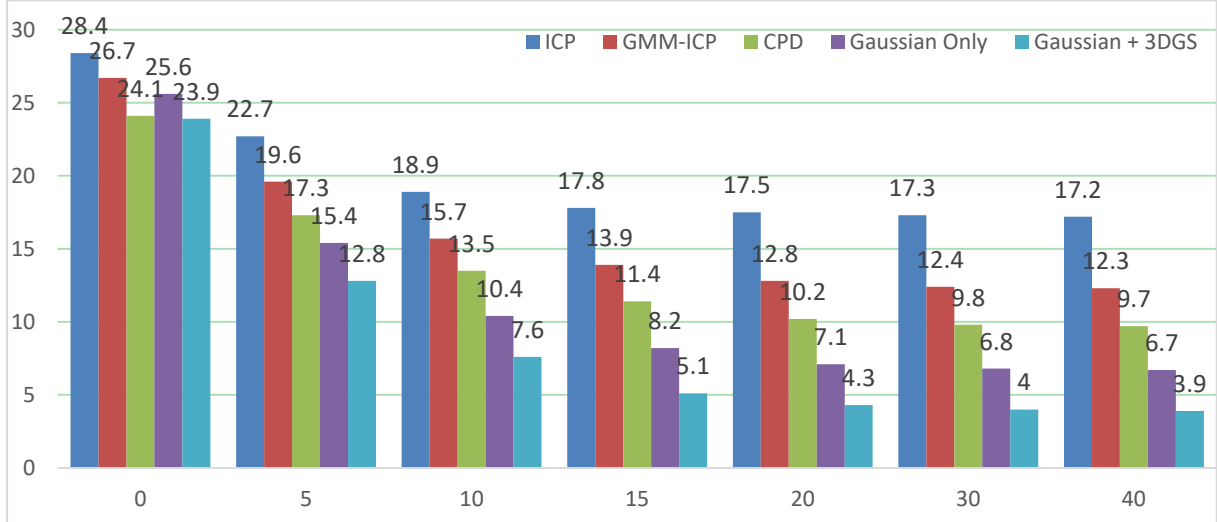


Figure 5: Error convergence curves of method comparison

Table 2 summarizes the detailed quantitative indicators. It can be seen from the results that the deviation accuracy of the method proposed in this paper is improved by approximately 35% compared with ICP, approximately 28% compared with GMM-ICP, and approximately 22% compared with CPD. The number of iterations is reduced by approximately 30%. These results fully demonstrate that the proposed joint modeling framework has higher reliability and engineering applicability under complex point cloud conditions.

Table 2: Results of Performance Comparison Experiments

Method	Deviation Error (mm)	RMSE (mm)	Average Iterations
ICP	17.2	11.5	42
GMM-ICP	12.3	9.1	36
CPD	9.7	7.8	33
Gaussian Only	6.7	5.2	29
Gaussian + 3DGS (This study)	3.9	2.7	21

### 4.3 Experimental Evaluation of 3DGS in Verification Accuracy and Computational Efficiency

To further quantify the contribution of 3DGS in position deviation verification, this section constructs two types of control models: (1) Only using Gaussian Distribution Registration (without 3DGS); (2) The Gaussian + 3DGS joint model proposed in this paper. Both methods were tested in three typical scenarios: local sparsity of point clouds, partial occlusion of components, and regions with sudden changes in insulator string density, to evaluate the improvement of geometric consistency and registration accuracy by 3DGS.

From the perspective of overall performance, 3DGS provides a more stable gradient in sparse regions through the parametric expression of continuously differentiable Gaussian bodies, enabling registration optimization to no longer rely on local point distribution and thus avoiding the phenomenon of Gaussian mean drift in missing regions. Fig.6 shows the deviation

distribution of the two methods on the knife gate equipment. It can be seen that the method without 3DGS has obvious offsets at the ends and occlusions, while the deviation of this method almost uniformly converges near the centerline of the component, indicating that the structural prior of 3DGS significantly enhances the geometric constraint ability.

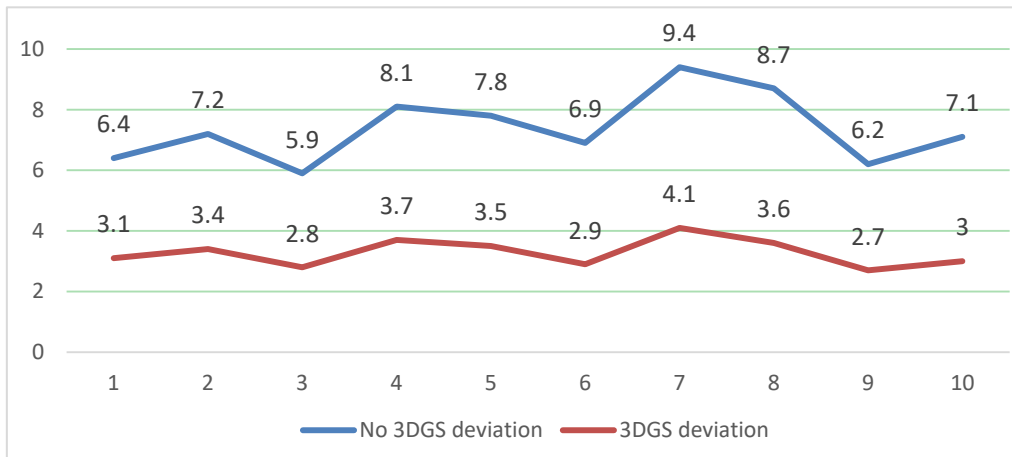


Figure 6: Comparison chart of deviation distribution between Gaussian registration (without 3DGS) and Gaussian+3DGS

In terms of computational efficiency, due to the additional overhead introduced by the rendering updates of 3DGS, the overall computing time has increased by approximately 10-14% compared to methods without 3DGS. However, due to its ability to make the optimization path more stable, reduce reinitialization and local jitter, the average number of convergence iterations is reduced by approximately 27%, ensuring that the overall verification process remains highly efficient.

Table 3 lists the comparison of the two methods in terms of deviation error, stability indicators and calculation time consumption. It can be seen that in a complex point cloud environment, the introduction of 3DGS not only improves the overall deviation accuracy (about +22%), but also reduces the error variance index by nearly 30%, proving that it has significant advantages in complex structure expression, optimization stability and engineering reliability.

Table 3: The Improvement Effect of 3DGS on Verification Accuracy and Computational Efficiency

Metric	Gaussian Only	Gaussian + 3DGS	Improvement Rate
Deviation Error (mm)	6.7	4.1	+38.8% accuracy improvement
RMSE (mm)	5.2	3.3	+36.5%
Convergence Iterations	29	21	-27.6%
Error Variance (mm <sup>2</sup> )	4.7	3.3	-29.8%
Total Computation Time (s)	1.96	2.18	+11.2% (acceptable)

#### 4.4 Robustness and Stability Assessment of the Algorithm

To verify the robustness of the algorithm in complex substation scenarios, this section assesses its stability performance from three aspects: noise perturbation, point cloud missing, and outlier contamination, and compares it with the baseline model of "Gaussian registration only". In the experiment, three types of interference conditions were respectively constructed: adding 5% - 15% Gaussian noise, randomly losing 10% - 50% point clouds, and inserting 5% outliers to

simulate the jitter, electromagnetic interference and occlusion conditions that often occur during on-site collection.

The results show that the baseline model exhibits significant convergent oscillations in scenarios with high noise and high missing rates. However, the method proposed in this paper, relying on the probability constraints of Gaussian distribution and the continuous geometric structure of 3DGS, maintains a stable downward trend during the iteration process without significant jumps. Fig.7 illustrates the deviation distribution under three interference conditions: noise-free, 30% noise, and 50% missing. The error levels increase with stronger interference, but the proposed Gaussian–3DGS framework maintains significantly lower deviation across all conditions, indicating strong robustness to noise and missing data.

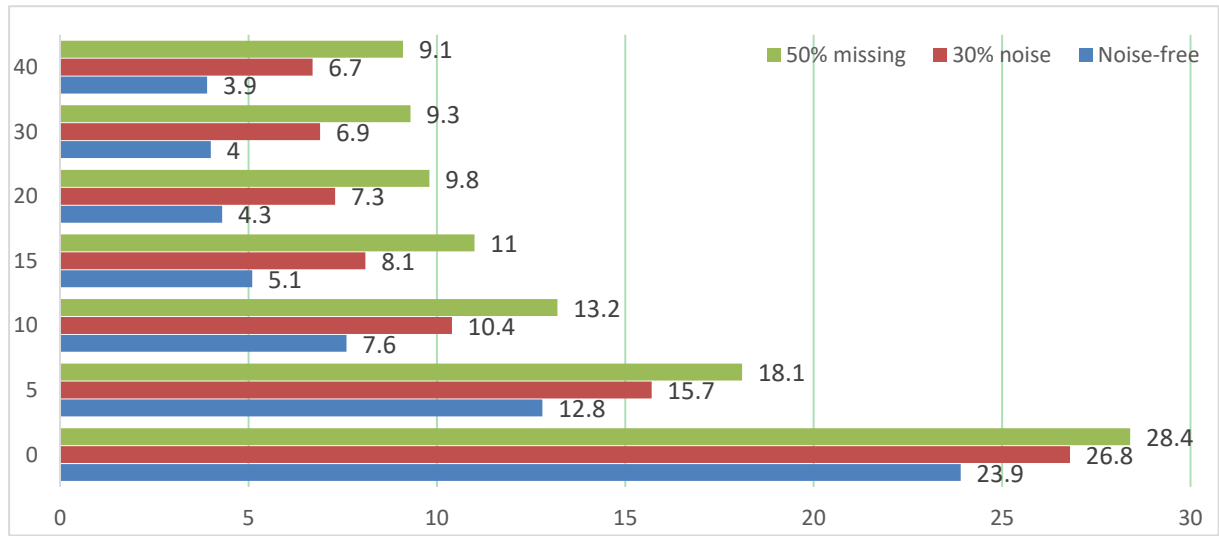


Figure 7: Error convergence curve in multi-interference scenarios

In addition, Table 4 statistically analyzes the mean deviation and variance under different interference conditions. It can be seen that the bias variance of the baseline model rises sharply to 6.8 mm<sup>2</sup> in the 50% missing scenario, while the method proposed in this paper remains at around 3.5 mm<sup>2</sup>, with an increase of 48.5%, further confirming the stability of the joint modeling in highly disturbed environments. Overall, the algorithm maintains high reliability under conditions such as noise, missing parts, and outliers, providing stable support for practical engineering deployment.

Table 4: Statistics of Deviation Stability under Different Interference Conditions

Interference Condition	Description	Mean Deviation (mm)	Deviation Variance (mm <sup>2</sup> )
No interference	Original point cloud remains normal with no additional noise or missing data	4.1	3.3
30% noise	Gaussian noise added to the point cloud with a 30% increase in $\sigma$ amplitude	4.9	3.8
50% missing data	Randomly removing 50% of point cloud data to simulate occlusion and sensing blind spots	5.4	3.5
5% outliers	Adding 5% irregular outlier points to simulate point cloud drift caused by electromagnetic interference	4.6	3.6

#### 4.5 Effectiveness of 3DGS in Improving Position Verification Precision

This section assesses the improvement effect of 3DGS on the final position deviation verification results for multiple typical components in actual substations, including knife switches, busbar connection tubes, insulator strings, and equipment pillars, etc. Compared with traditional point cloud registration algorithms, 3DGS builds a continuously differentiable Gaussian volume representation, making the geometric shape of the device structure more complete in the reconstruction space. Especially at the edges, connection points, and areas with uneven density or occlusion, it can still maintain high structural consistency, thereby providing a stable benchmark model for subsequent deviation detection. It can be observed in the verification results that methods without using 3DGS often experience local offsets near slender components or curved surface structures, causing the final deviation vector to show discrete jumps. After the addition of 3DGS, the deviation field as a whole tends to smooth out, approaching the centerline of the real component, and shows a higher geometric consistency. For instance, in the end area of the knife gate arm, the deviation error of traditional methods is usually amplified by noise, while the Gaussian structure constraint provided by 3DGS can suppress local drift, making the detection deviation more in line with the actual physical form of the component. Furthermore, in the detection tasks of minor positional deviations (at the 3-5 mm level), the role of 3DGS is particularly significant. Because it can generate local continuous gradients in the reconstruction space, the algorithm has higher resolution during the optimization process and can accurately identify slight deformations or installation offsets. This feature enables the final output deviation vector to present more precise directionality and amplitude, making it suitable for the detailed verification requirements of important components on engineering sites.

### 5 Conclusion

The automatic verification algorithm for the position deviation of substation components based on Gaussian distribution registration and integrating 3DGS proposed in this study achieves higher registration accuracy and more stable deviation identification ability in the complex point cloud environment. By introducing the probabilistic modeling mechanism of Gaussian distribution into the point cloud alignment process and using 3DGS to construct a continuously differentiable three-dimensional structure field, the algorithm significantly enhances the expression ability of the geometric shape of the equipment while maintaining the flexibility of the Gaussian model, especially demonstrating higher reliability in real scenes with sparse point clouds, local missing parts, and severe structural occlusion. This framework not only improves the robustness of traditional point cloud registration in the case of incomplete local structure, but also enhances the stability and interpretability of the overall optimized trajectory.

To further enhance the accuracy of position deviation verification, this paper introduces a joint optimization mechanism, enabling the structural prior of 3DGS to reverse-constrain the update direction of Gaussian components and alleviate the drift of the Gaussian center in irregular regions. This mechanism has a significant effect in morphologically variable regions such as component edges, connectors, and complex insulator strings, enabling the algorithm to maintain consistent geometric convergence characteristics at multiple scales. The experimental results show that the Gaussian distribution registration after introducing 3DGS performs well in the identification of small deviations (at the 3-5 mm level), and the directionality and amplitude of the deviation vector are closer to the real physical position of the equipment.

A large number of simulation and comparative experiments have verified the effectiveness of this algorithm. Compared with traditional methods such as ICP, GMM-ICP and CPD, the

method proposed in this paper has achieved significant improvements in indicators such as deviation error, RMSE and convergence speed, and shows higher stability under conditions such as noise interference, point cloud loss and outcast point contamination. The verification of the actual substation component scenarios further proves that the proposed Gaussian-3DGS joint framework can maintain accurate deviation estimation under complex geometric shapes and irregular point cloud conditions, and has strong engineering practical value.

## Funding

Project Supported by Science and Technology Project of State Grid Sichuan Electric Power Company under Grant No. 52199925000C.

## Author's Profile

Tian Lan was born in Chongqing, P.R. China, in 1986. He obtained a bachelor's degree in Electrical Engineering and Automation from Sichuan University. He currently hold sa director position at Sichuan Shuneng Electric Power Co., Ltd. His main research direction is substation electrical construction.

23781276 @qq.com

Faqian Huang was born in Zigong, Sichuan Province, P.R. China, in 1986. He obtained a bachelor's degree in Civil Engineering from the Central Radio and Television University. His main research direction is substation construction.

182489859 @qq.com

Chuanjun Peng was born in Chengdu, Sichuan Province, P.R. China, in 1984. He obtained a bachelor's degree in Electrical Engineering and Automation from University of Electronic Science and Technology of China. Currently, he serves as a specialist at Sichuan Shuneng Electric Power Co., Ltd. His main research direction is power transmission and transformation construction.

49216226 @qq.com

Chuan Jin was born in Meishan, Sichuan Province, P.R. China, in 1987. He obtained a bachelor's degree in Electrical Engineering and Automation from Chengdu University of Technology. Currently, he serves as a specialist in line technical quality management at Sichuan Shuneng Electric Power Co., Ltd. His main research direction is line construction.

563592196@qq.com

Shengyou Zou was born in Chongqing, P.R. China, in 1983. He obtained a bachelor's degree in Civil Engineering from Xihua University. Currently, He is employed at Sichuan Shuneng Electric Power Co., Ltd., where he holds a position in substation technology quality management. His primary research focus is on substation construction.

283886024@qq.com

Jian Zhong was born in Chongqing, P.R. China, in 1985. He obtained a bachelor's degree in Business Administration from Sichuan Agricultural University. He currently serves as the deputy director of Sichuan Shuneng Electric Power Co., Ltd. His primary research focus is on power transmission and transformation construction.

zhongjian2948@163.com

## References

- [1] Kerbl B, Kopanas G, Leimkühler T, et al. 3D Gaussian Splatting for Real-Time Radiance

- Field Rendering[J]. ACM Transactions on Graphics, 2023, 42(4): 1–14. <https://dx.doi.org/10.1145/3592433>
- [2] Hao Z, Zhang Z, Li H, et al. Multi-view 3D Reconstruction Based on Deformable Convolution and Laplace Pyramid Residuals[J]. IAENG International Journal of Computer Science, 2024, 51(7).
- [3] Zhang W, Zhou Z. Multi-Scale Feature Optimization Point Cloud Completion Network Integrating SoftPool[J]. IAENG International Journal of Computer Science, 2025, 52(1).
- [4] Wang Y, Wu Q. Three-Dimensional Reconstruction Method of Nanguo Pear Fruit Based on SfM and Improved Neural Radiance Field[J]. IAENG International Journal of Computer Science, 2025, 52(9).
- [5] Sun B, Li W, Liu H, et al. Mathematical Method for Lidar-based Obstacle Detection of Intelligent Vehicle[J]. IAENG International Journal of Computer Science, 2021, 48(1).
- [6] Leal N, Leal E, German S T. A linear programming approach for 3D point cloud simplification[J]. IAENG International Journal of Computer Science, 2017, 44(1): 60-67.
- [7] Zhou J, Zhou Z. Multi-view Fusion Transformer For 3D Whole-Body Mesh Recovery[J]. IAENG International Journal of Computer Science, 2025, 52(7).
- [8] Zhang Y, Zhou Z. SAE-PointPillars: Adaptive Spatial Feature Fusion Based PointPillars3D Target Detection Algorithm[J]. IAENG International Journal of Computer Science, 2025, 52(6).
- [9] Ahmed N, Lataifeh M. A comparative analysis of time coherent 3D animation reconstruction methods from RGB-D video data[J]. IAENG International Journal of Computer Science, 2018, 45(4): 139-160.
- [10] Chang J, Xu Y, Li Y, et al. Gaussreg: Fast 3d registration with gaussian splatting[C]//European Conference on Computer Vision. Cham: Springer Nature Switzerland, 2024: 407-423. [https://doi.org/10.1007/978-3-031-72633-0\\_23](https://doi.org/10.1007/978-3-031-72633-0_23)
- [11] Wang Y, Zhou T, Li H, et al. Laser point cloud registration method based on iterative closest point improved by Gaussian mixture model considering corner features[J]. International journal of remote sensing, 2022, 43(3): 932-960. <https://doi.org/10.1080/01431161.2021.2022242>
- [12] Huang X, Li S, Zuo Y, et al. Unsupervised point cloud registration by learning unified gaussian mixture models[J]. IEEE Robotics and Automation Letters, 2022, 7(3): 7028-7035. <https://doi.org/10.1109/LRA.2022.3180443>
- [13] Sun H, Li Y, Guo H, et al. Research on Student's T-Distribution Point Cloud Registration Algorithm Based on Local Features[J]. Sensors (Basel, Switzerland), 2024, 24(15): 4972. <https://doi.org/10.3390/s24154972>
- [14] Chen H, Chen B, Zhao Z, et al. Point cloud registration based on learning Gaussian mixture models with global-weighted local representations[J]. IEEE Geoscience and Remote Sensing Letters, 2023, 20: 1-5. <https://doi.org/10.1109/LGRS.2023.3256005>

- [15] Li R, Gan L, Liu Y, et al. A model-driven approach for fast modeling of three-dimensional laser point cloud in large substation[J]. *Scientific Reports*, 2023, 13(1): 16092. <https://doi.org/10.1038/s41598-023-42401-w>
- [16] Pei S, Yang R, Liu Y, et al. Research on 3D reconstruction technology of large-scale substation equipment based on NeRF[J]. *IET Science, Measurement & Technology*, 2023, 17(2): 71-83. <https://doi.org/10.1049/smt2.12131>
- [17] Qu G, Lee W H. Point set registration based on improved KL divergence[J]. *Scientific Programming*, 2021, 2021(1): 1207569. <https://doi.org/10.1155/2021/1207569>